THE ASTROPHYSICAL JOURNAL SUPPLEMENT SERIES, 120:171–178, 1999 February

CALTECH FAINT GALAXY REDSHIFT SURVEY. VII. DATA ANALYSIS TECHNIQUES AND REDSHIFTS IN THE FIELD J0053+1234[1]

JUDITH G. COHEN,[2] DAVID W. HOGG,[3,4,5] MICHAEL A. PAHRE,[2,5,6] ROGER BLANDFORD,[3]
PATRICK L. SHOPBELL,[2] AND KEVIN RICHBERG[2]
Received 1998 June 11; accepted 1998 September 17

ABSTRACT

We present the techniques used to determine redshifts and to characterize the spectra of objects in the Caltech Faint Galaxy Redshift Survey in terms of spectral classes and redshift quality classes. These are then applied to spectra from an investigation of a complete sample of objects with $K_s < 20$ mag in a 2×7.3 arcmin^2 field at J005325+1234. Redshifts were successfully obtained for 163 of the 195 objects in the sample; these redshifts lie in the range [0.173, 1.44] and have a median of 0.58 (excluding 24 Galactic stars). The sample includes two broad-lined AGNs and one QSO.

Subject headings: cosmology: observations — galaxies: distances and redshifts — surveys

1. INTRODUCTION

The Caltech Faint Galaxy Redshift Survey, (CFGRS), is designed to measure the properties of field galaxies in the redshift interval $0.3 \lesssim z \lesssim 1.3$. It uses complete samples to a fixed limiting magnitude in a particular bandpass within a small solid angle on the sky. Spectra are obtained for every object in the sample with the Low Resolution Imaging Spectrograph (LRIS) (Oke et al. 1995) on the 10 m Keck Telescope. The defining features of this program that distinguish it from existing and ongoing or planned surveys, such as the CfA1 Survey (Huchra et al. 1983), the Las Campanas Redshift Survey (Shectman et al. 1996), the Canada-France Redshift Survey (CFRS; Lilly et al. 1995a, 1995b), the Autofib survey (Ellis et al. 1996), the Century Survey (Geller et al. 1997), the ESO slice survey (Vettolani et al. 1997), the Sloan Digital Sky Survey (Gunn & Knapp 1993), the Deep Survey planned by the Lick group (Koo 1998), and the 2dF Survey (Colless & Boyle 1998), are that it is possible to reach to fainter magnitudes ($K \sim 20$ mag, $R \sim 24$ mag) and that completeness is emphasized rather than sparse sampling over a large field. The closest counterpart to this approach is the work of Cowie et al. (1996), although we note that the present survey covers a larger solid angle at the survey limit. See Koo & Kron (1992) and Ellis (1997) for reviews of the subject.

There are four limitations to "pencil beam" redshift surveys of the type described in the present paper when addressing issues of galaxy evolution. The first is that the faintest fluxes at which sources can be observed in a complete redshift survey are still over 4 mag brighter than the fluxes of the faintest detectable sources in imaging data. The second is that the total number of sources and total sky area are both limited by available telescope time because the faintest possible sources are being studied. This is particularly relevant to attempts to characterize large-scale structure. The third is that it is difficult to measure spectroscopic redshifts in the range $1.3 < z < 2.3$—the lower limit is set by the [O II] line at 3727 Å moving out of the optical regime, the upper limit by when Lyα enters it. This may be a crucial period in the formation and evolution of normal galaxies (Madau, Pozzetti, & Dickinson 1998). The final limitation is the difficulty of generalizing the observed properties in a small field (which may contain unique features) to the properties of the field galaxy population as a whole.

This paper presents spectroscopic results from one field located at J005325+1234, the central region of which is part of the Medium Deep Survey (Griffiths et al. 1994) and among the deepest fields imaged with *HST* prior to the Hubble deep field. The field measures 2×7.3 arcmin^2 with a statistical sample containing 195 infrared-selected objects complete to $K = 20$ mag, of which 24 are spectroscopically confirmed Galactic stars and 32 cannot be assigned spectroscopic redshifts. (21 of these have spectra). There are 13 additional objects with redshifts (including two more stars) that are just outside the field boundary or are within the field but too faint.

This paper is structured as follows. The sample is defined in § 2, which is followed by a description of the spectroscopic observations and redshift determinations in § 3. The galaxy spectra are assigned to spectroscopic and quality classes, a procedure discussed in § 4.

2. SAMPLE DEFINITION

The sample, defined in Pahre et al. (1998), is selected by the criteria that $K_s < 20$ mag within a 2×7.3 arcmin^2 field centered at $00^h53^m23^s.20$ $+12°33'58''$ (J2000). In an effort to cut down the thermal background of the standard Johnson K filter, which has a central wavelength 2.2 μm and FWHM 0.4 μm, there are at least two nonstandard filters in this same atmospheric window in common use: the K' filter of Wainscoat & Cowie (1992) and the K_s (K-short) filter of Persson (1998, private communication) and Skrutskie et al. (1999). The latter is used here and covers at half-maximum transmission the wavelength range $2.00 < \lambda < 2.32$ μm. Throughout this series of papers, unless otherwise specified, we use K (denoting the standard Johnson filter) and K_s (denoting the K-short filter) interchangeably, although the appropriate K_s transmission curve is used when deriving the k-corrections in Cohen et al. (1998).

[1] Based in large part on observations obtained at the W. M. Keck Observatory, which is operated jointly by the California Institute of Technology and the University of California.

[2] Palomar Observatory, Mail Stop 105-24, California Institute of Technology, Pasadena, CA 91125.

[3] Theoretical Astrophysics, California Institute of Technology, Mail Stop 130-33, Pasadena, CA 91125.

[4] Current Address: Institute for Advanced Study, Olden Lane, Princeton, NJ 08540.

[5] Hubble Fellow.

[6] Current Address: Harvard-Smithsonian Center for Astrophysics, 60 Garden Street, Mail Stop 20, Cambridge, MA 02138.

This sample contains 195 objects, and we refer to this as the "main" sample. It includes 24 spectroscopically confirmed Galactic stars. The remaining 171 objects constitute the "galaxy" sample. We were able to assign redshifts to 139 of these galaxies, and this is the "redshift" sample. Redshifts were also obtained for several objects that either had $K > 20$ mag or lie just outside the boundary of the sample. A few objects that are very faint at both R and K turned up serendipitously in slitlets intended for nearby brighter objects. Adding these 13 additional objects to the main sample defines the "total" sample of 208.

The photometric data of Pahre et al. (1998) are already corrected for reddening by the ISM in the Galaxy. The variation in $E(B-V)$ across the small field of our survey is insignificant. As is conventional, we ignore reddening internal to the galaxies themselves and from the IGM.

3. REDSHIFT DETERMINATIONS

3.1. *Data Acquisition and Reduction*

The objects in this sample were observed using the LRIS at the Keck Observatory beginning in 1994 October and ending in 1998 January. The LRIS detector is a 2048×2048 pixel Tektronix CCD. Its dual amplifier readout mode was normally used to save time. Observations were carried out even when the weather was not photometric. Fifteen slit masks were used. Each mask has 25 to 33 slitlets and many objects were observed more than once. A few of the brightest galaxies were selected as aids to align the masks, and hence were observed many times.

Except for the last three masks (the 1997 and 1998 data), the 300 g mm^{-1} grating was used with 1.″1 wide slits. This produces a scale of 2.46 Å pixel^{-1} and a resolution of 10 Å. (This is ~ 4 times higher spectral resolution than that of the CFRS.) The spectral coverage is ~ 5000 Å, with the central wavelength depending on the location of the object on the sky with respect to the center line of the slit mask as well as on the grating tilt. Two 3000 s exposures were obtained for each of these masks.

The last three masks, containing most of the faintest objects in the sample, were observed with the 155 g mm^{-1} grating with 1.″0 wide slits giving a spectral resolution of 20 Å. Two or three 1800 s exposures were obtained for each of these slit masks. Each of these lower dispersion spectra was slightly shifted in central wavelength (i.e., dithered spectrally between exposures). This forces a more complex reduction, but better signal-to-noise spectra are achieved. Full spectral coverage from the UV through 10000 Å is achieved with this grating for essentially all objects at the price of lower dispersion.

These multislit spectra were reduced in a standard way. The bias (actually right and left amplifier bias levels) was subtracted. Then, the relevant pieces were cut out of each of the multislit spectra for a particular object (and out of the flat field calibration exposure), cosmic rays were removed, the subsets were flattened, and the bowing of the spectra (the S-distortion) was removed. When necessary, the distortion in the vertical direction along the slit that manifests itself as tilted night sky lines was also removed.

The night sky lines within the spectra themselves were used to define the wavelength scale; a third-order polynomial fit is sufficient. This means in effect that there are no "arc" lines bluer than 5199 Å. Sometimes that night sky emission line could not be detected, in which case 5577 Å became the bluest night sky line. Sky subtraction was accomplished by fitting a second order polynomial to a range of pixels above and below the object spectrum. Linear fits were used when necessary, particularly when the object was near the top or bottom edge of the slitlet.

The spectra were reduced by J. G. C. using Figaro (Shortridge 1988) scripts and about 20% were also done by D. W. H. using IRAF[7] scripts. J. G. C. measured all the redshifts uniformly, including remeasurement and in some cases rereduction of the spectra done by D. W. H. as well. The redshifts were measured by visually determining the wavelengths of spectral features from plots of the spectra over various wavelength ranges on an interactive display. The assignment of rest wavelengths to the observed spectral features was straightforward for the brighter objects and for those objects with strong emission lines, but it became more difficult for the faint objects showing only absorption line spectra.

While a manual redshift determination may seem outmoded in light of more automatic techniques such as that developed by Glazebrook, Offer, & Deeley (1998) for the 2dF or that of Kurtz & Mink (1998) for the CfA surveys, in this situation it is more appropriate. Here the objects are very faint relative to the background sky, the SNR is low, the sky subtraction is difficult, the exposures are long (thus increasing the number of cosmic-ray hits), and most importantly we do not fully understand what features to expect in the spectra of such faint and distant galaxies. Construction of a set of templates for a machine based redshift search from (or even for) this data set would be impossible.

The spectra have been fluxed using long-slit observations of standard stars from Oke (1990) taken with the same LRIS configuration as was used for the multislits. The absolute scale of a fluxed spectrum should be regarded with caution, as the nights were not all photometric, there are substantial slit losses for the more extended objects, and slit mask alignment causes an additional light loss that is variable from mask to mask and from object to object on a given mask. However, the *shape* of the continuum for a particular object should be more or less correct and is often quite useful.

3.2. *Redshift Measurements*

Redshifts were measured for each object in each of the slit masks. Records were also kept of the results for any serendipitous objects that fell onto slits for other targeted galaxies. At the end, the results were compiled, and the very small number of objects with multiple observations that showed discrepancies were studied more carefully to resolve them. This involved summing all the spectra together, examining the wavelength range of each of the spectra, etc.

The most difficult cases involved objects that show no emission features, but only absorption lines which do not correspond to the standard pattern of Balmer lines, H + K Ca II doublet, etc., seen in the region of the 4000 Å break. Since the 4000 Å region is redshifted into the strong night sky emission lines redward of the optical bandpass for $z > 1$, it was suspected that for such objects $z > 1$. To deal with these particular cases, the spectra were compared

[7] IRAF is distributed by the National Optical Astronomy Observatories, which is operated by the Association of Universities for Research in Astronomy, Inc. (AURA) under cooperative agreement with the National Science Foundation.

TABLE 1

REDSHIFT QUALITY CLASSES

Quality Class	Description of Class
1	Multiple features, $\sigma(z) \leq 0.002$/feature
2	Multiple features, $\sigma(z) \leq 0.004$/feature
3	Multiple features, faint, id uncertain, $\sigma(z)$ small 75% of time, and wildly off 25% of time
4	One emission line only, solid, assume 3727 Å
5	One emission line only, reality uncertain, assume 3727 Å
6	Multiple features, at least one broad emission line
7	Only one broad emission line, assumed to be 2800 Å
8	Single break, assumed to be 4000 Å break
9	Single strong absorption feature, assumed to be 2800 Å because of shape of continuum
0	No redshift

directly with spectra of high-redshift galaxies (Cowie, Hu, & Songaila 1995; Steidel et al. 1996), the sum of spectra of absorption line galaxies in a cluster at $z = 1.50$ kindly supplied by J. B. Oke, as well as the sums of spectra of galaxies in the higher redshift peaks in the present sample. The library of mean ultraviolet spectral energy distributions for stellar groups from *IUE* spectra (Fanelli et al. 1992) and those of model galaxies from the grid of Bruzual & Charlot (1993) were also examined.

The absorption features in the spectra of many of those objects suspected to be at $z > 1$ are real and repeatable. The uncertainty in the redshifts is because of limited knowledge of this spectral region (for which the 2800 Å region is shifted into the optical) and lack of confidence when there are only two certain features in a spectrum, both absorption lines, as to what the correct identification should be. A good example is D0K42 (which has $R_{\rm obs} = 23.12$, $R - K = 5.14$), which could have either $z = 0.54$ or the final adopted value of $z = 1.14$ depending on whether the identification assigned to the strongest absorption features is H + K of Ca II or 2800 + 2850 Å (Mg II + Mg I). In this case, the spectral energy distribution of the fluxed spectra and the absence of a 4000 Å jump in the $z = 0.54$ case were considered to be persuasive evidence for the higher value.

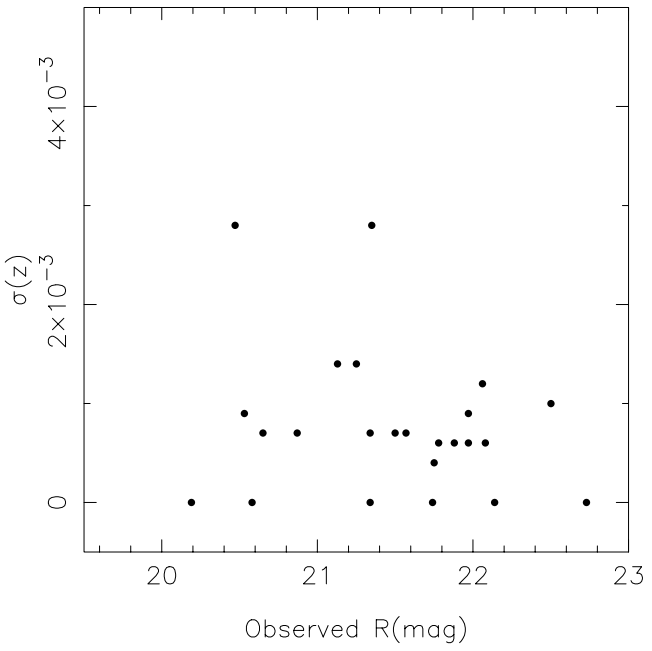

FIG. 1.—The rms dispersion in redshift is shown for galaxies with multiple spectra as a function of R magnitude. The implied scatter for a single redshift measurement is ~0.0008.

The composite quasar spectrum of Francis et al. (1991) provided a template for line identification in the broad emission line objects.

3.3. *Quality Classes*

We assign a quality class to the redshift of each object to give an indication of the associated uncertainty. Table 1 lists the quality classes (0 through 9) with a brief description of each. Objects with multiple features are assigned quality class 1–3 redshifts, depending upon the security of the redshift. Centroiding uncertainties for high SNR spectra are generally considered to be less than 0.1 × FWHM, but with the lower SNR prevalent here, we adopt a FWHM as a more appropriate uncertainty. (The uncertainty from the wavelength fit itself using the night sky lines is small by comparison.) For a feature at 6000 Å with $z < 1.5$, a 2 pixel error with the 300 g mm^{-1} grating corresponds to a redshift uncertainty ≤ 0.002.

Single emission line spectra are placed in classes 4 and 5. The emission line is always assumed to be 3727 Å [O II]. The CFRS has adopted a similar strategy (Lilly et al. 1995a), although their situation is more complex as they are more likely to have confusion between 3727 Å emission and Hα emission due to the preponderance of lower redshift galaxies in the CFRS. In our case, with our relatively broad spectral coverage, the absence of Hβ or 4959 Å emission serves to rule out the possibility that a single emission line is 5007 Å of [O III]. It cannot be Hα for lines that appear at wavelengths bluer than the rest wavelength of Hα, while for redder lines, one would then expect to see Hβ or the 5007 Å [O III] line in emission. The only other serious possibility consistent with the absence of features in optical spectra with broad spectral coverage is Lyα; this is a serious possibility for some of the faintest objects in the sample, particularly the serendipitous ones, where only a single emission line from a very faint object falls by chance onto our slit, cf. Dey et al. (1998). In such cases, broadband colors might be used to look for breaks or UV dropouts, although we have chosen to assign redshifts on the basis of spectroscopy alone. The presence of a few high-redshift objects in our sample should not affect our conclusions, which are restricted to the properties of galaxies with $z < 1.5$.

Objects showing a single break, assumed to be the 4000 Å break, are assigned quality class 8. Again this is a conservative choice, since at a modest redshift well within the range

TABLE 2

DEFINITION OF SPECTRAL TYPES

Spectral Type	Defining Features
	Galactic Stars
$\mathscr{M}$	TiO bands (M dwarfs); CaH bands (M subdwarfs)
$\mathscr{S}$	Absorption in Mg triplet, Balmer lines
$\mathscr{W}$	White dwarf, broad Balmer line absorption
	Extragalactic Objects
$\mathscr{Q}$	At least one broad emission line
$\mathscr{B}$	Emission in Hδ and Hϵ as well as 3727, Hβ, 5007
$\mathscr{E}$	Dominated by emission lines, 3727, 5007
$\mathscr{C}$	Composite, 3727 + Balmer line absorption
$\mathscr{A}$	No emission lines, only absorption features
	Unknown Objects
$\mathscr{F}$	Observed, but no redshift
$\mathscr{U}$	Never observed spectroscopically

covered by our survey, the break just to the red of the Mg II doublet at 2800 Å will lie in the optical. There are only two objects in this class in the total sample. Quality class 9 is for objects showing a single strong absorption feature that, because of the shape of the continuum, we interpret as Mg II + Mg I at 2800 + 2850 Å rather than as Ca H + K. There are only three such objects.

Quality class 0 is for objects with very low signal and no redshift.

For future reference, the term "high-quality redshifts" refers to those with a quality class indicating a secure z, specifically quality classes 1, 2, 4, or 6.

To demonstrate that the quality class 1 spectra (which comprise more than 50% of the extragalactic objects) actually do have the precision claimed above, Figure 1 shows the values of σ calculated from multiple spectra of a single object where each individual measurement has a quality 1 rating as a function of R magnitude. Only the galaxies with multiple spectra among the 60 brightest

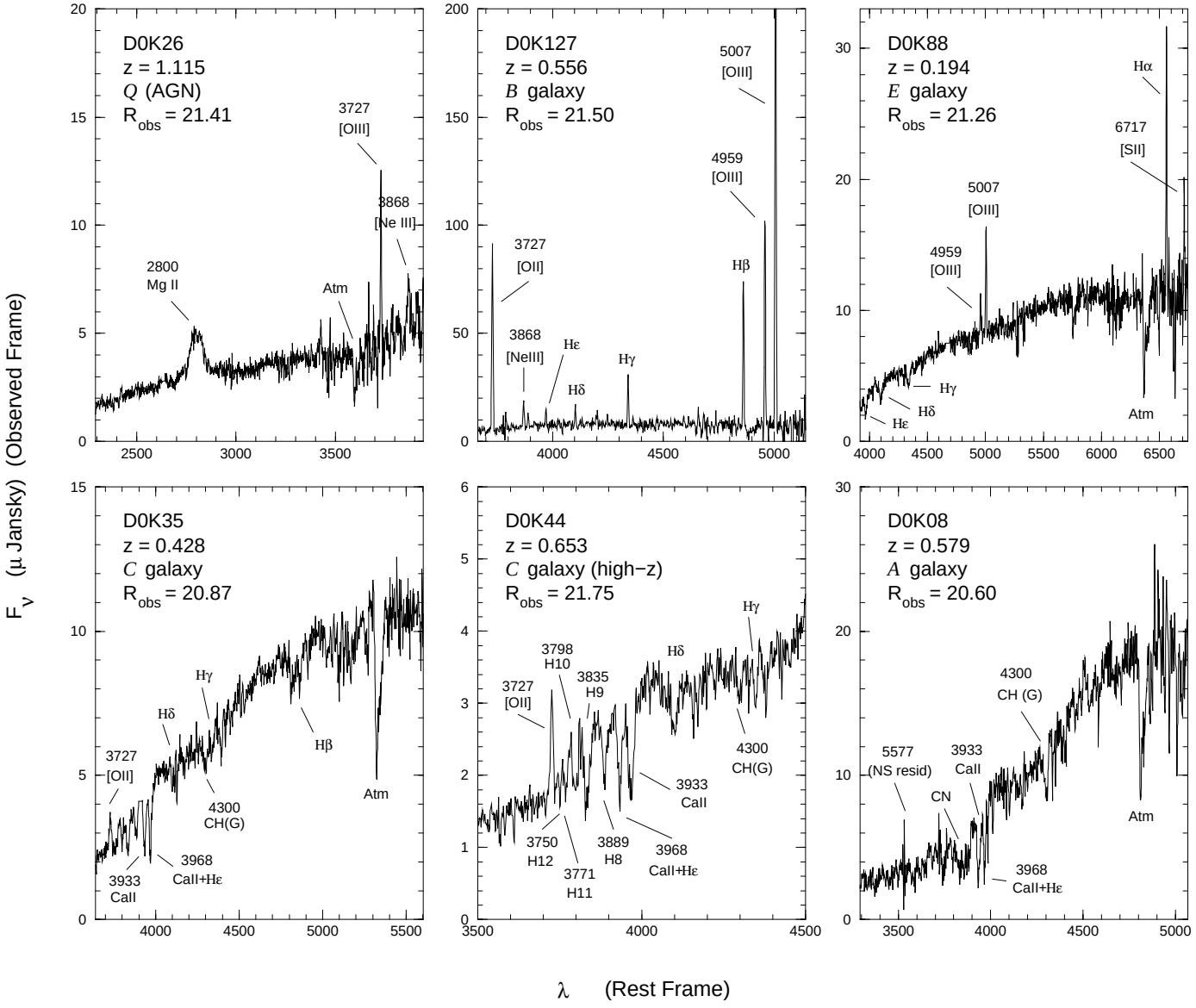

FIG. 2.—Representative spectra of each of the five spectral classes assigned to extragalactic objects are shown. The spectrum of the second brightest AGN and the second brightest starburst galaxy is shown, while the fifth brightest galaxy in R is shown for each of the other three spectral classes. The spectrum of a high-z "$\mathscr{C}$" galaxy is also shown.

TABLE 3

SURVEY OBJECTS

ID (D0K)	R.A.[a] (−0[h])	Decl. (−12°)	K (mag)	z	QC	SC	ID (D0K)	R.A.[a] (−0[h])	Decl. (−12°)	K (mag)	z	QC	SC
Main Sample													
1	5327.93	3018.40	12.73	0.000	1	*M*	2	5327.69	3214.60	14.43	0.000	1	*S*
3	5322.88	3546.60	14.91	0.000	1	*S*	4	5322.94	3352.90	15.38	0.000	1	*M*
5	5328.48	3717.70	15.58	0.000	1	*M*	6	5328.72	3029.50	15.68	0.428	1	*A*
7	5328.48	3731.40	15.87	0.000	1	*S*	8	5327.87	3332.50	16.27	0.579	1	*A*
9	5327.94	3613.70	16.30	0.441	1	*C*	10	5325.61	3718.90	16.49	0.000	1	*M*
11	5323.82	3729.90	16.67	0.346	1	*A*	12	5324.73	3342.40	16.75	0.681	6	*Q*
13	5324.12	3027.40	16.83	0.588	1	*C*	14	5325.89	3536.90	16.88	0.428	1	*A*
15	5324.55	3732.00	16.89	0.000	1	*M*	16	5328.16	3044.40	16.95	0.431	1	*A*
17	5322.22	3209.90	16.98	0.392	1	*A*	18	5322.56	3252.30	17.02	0.173	1	*C*
19	5325.95	3151.20	17.02	0.581	1	*A*	20	5324.71	3437.80	17.10	0.000	1	*M*
21	5327.85	3652.30	17.13	0.000	1	*M*	22	5325.87	3144.90	17.14	0.581	1	*A*
23	5323.46	3415.40	17.21	0.000	1	*M*	24	5325.94	3423.30	17.30	0.679	1	*C*
25	5324.24	3639.40	17.39	0.309	1	*C*	26	5322.37	3059.00	17.44	1.115	6	*Q*
27	5326.13	3147.80	17.44	0.577	1	*A*	28	5324.43	3409.10	17.44	0.582	1	*A*
29	5326.30	3239.20	17.45	0.582	1	*AC*	30	5328.38	3501.80	17.52	0.621	1	*C*
31	5329.12	3222.70	17.53	0.430	1	*A*	32	5329.32	3330.10	17.54	0.577	1	*A*
33	5325.91	3558.40	17.54	0.429	1	*A*	34	5324.73	3411.80	17.55	0.679	1	*AC*
35	5329.07	3457.20	17.56	0.428	1	*C*	36	5323.73	3711.00	17.58	0.605	1	*AC*
37	5326.88	3634.40	17.69	0.772	1	*A*	38	5327.08	3610.40	17.75	0.763	1	*A*
39	5323.21	3328.60	17.75	0.583	1	*C*	40	5324.94	3202.30	17.80	0.582	1	*A*
41	5322.00	3303.90	17.82	0.654	1	*AC*	42	5327.65	3522.40	17.82	1.136	3	*A*
43	5321.79	3018.00	17.86	0.000	1	*M*	44	5321.92	3320.30	17.88	0.653	1	*C*
45	5325.90	3158.70	17.88	0.581	1	*A*	46	5325.50	3047.30	17.91	0.763	1	*C*
47	5324.59	3347.00	17.99	0.582	1	*C*	48	5327.76	3545.30	18.00	0.578	2	*C*
49	5323.74	3441.70	18.06	0.584	1	*C*	50	5323.10	3234.50	18.08	0.000	1	*M*
51	5321.54	3135.40	18.09	0.677	1	*C*	52	5327.78	3457.30	18.10	0.680	1	*C*
53	5329.39	3307.20	18.10	0.000	1	*S*	54	5328.49	3724.10	18.11	0.209	1	*EC*
55	5324.02	3336.60	18.13	0.432	1	*C*	56	5325.90	3229.60	18.27	0.689	3	*A*
57	5327.08	3132.00	18.28	0.369	1	*EB*	58	5328.86	3251.90	18.28	0.509	1	*C*
59	5322.50	3549.70	18.29	0.771	1	*C*	60	5329.13	3719.00	18.30	0.781	3	*A*
61	5326.73	3650.20	18.32	0.000	1	*S*	62	5327.54	3417.70	18.34	0.584	2	*A*
63	5321.73	3141.00	18.35	0.535	3	*C*	64	5324.50	3701.90	18.42	1.048	3	*A*
65	5326.91	3051.30	18.44	1.232	3	*A*	66	5325.60	3243.90	18.46	0.771	1	*EC*
67	5327.95	3255.90	18.46	0.584	1	*A*	68	5321.40	3153.70	18.47	1.392	2	*A*
69	5321.32	3514.40	18.51	1.336	3	*A*	70	5328.97	3156.00	18.54	0.581	1	*A*
71	5323.70	3634.50	18.54	0.209	1	*E*	72	5321.96	3341.10	18.56	...	0	*F*
73	5326.51	3419.00	18.57	0.493	1	*C*	74	5321.62	3117.90	18.60	0.676	2	*C*
75	5322.20	3658.30	18.60	0.763	1	*C*	76	5322.76	3155.00	18.63	1.153	6	*Q*
77	5325.63	3510.80	18.64	...	0	*F*	78	5329.70	3104.30	18.66	0.633	1	*B*
79	5321.35	3346.80	18.68	0.533	1	*A*	80	5325.68	3444.50	18.74	0.585	2	*C*
81	5326.81	3030.10	18.75	0.414	1	*C*	82	5323.64	3343.70	18.76	0.000	1	*M*
83	5321.70	3426.30	18.80	0.429	1	*C*	84	5326.45	3359.20	18.81	0.678	1	*C*
85	5326.15	3350.40	18.81	0.626	1	*C*	86	5324.44	3515.60	18.82	0.549	1	*E*
87	5327.41	3308.50	18.82	0.440	1	*E*	88	5327.26	3627.90	18.85	0.194	1	*E*
89	5325.48	3108.40	18.86	0.581	1	*A*	90	5328.99	3442.40	18.87	0.511	1	*C*
91	5324.24	3709.00	18.88	...	0	*F*	92	5324.11	3645.90	18.89	0.000	1	*M*
93	5322.02	3216.60	18.90	1.043	2	*A*	94	5322.52	3732.00	18.91	...	0	*F*
95	5326.78	3626.20	18.91	0.000	1	*M*	96	5324.18	3020.20	18.94	0.677	1	*C*
97	5328.80	3434.70	18.94	0.531	8	*A*	98	5322.04	3045.50	18.97	...	0	*F*
99	5324.95	3035.40	18.98	0.000	1	*M*	100.....	5326.95	3552.90	19.00	0.680	2	*C*
101.....	5325.93	3214.10	19.01	0.578	1	*A*	102.....	5323.44	3336.00	19.01	0.448	3	*A*
103.....	5321.72	3038.80	19.01	0.607	1	*EC*	104.....	5323.46	3558.00	19.05	0.182	1	*B*
105.....	5328.83	3334.80	19.05	0.681	1	*E*	106.....	5322.29	3646.70	19.06	...	0	*U*
107.....	5324.77	3148.00	19.10	...	0	*F*	108.....	5328.14	3527.30	19.13	1.013	1	*E*
109.....	5321.56	3607.60	19.15	0.000	1	*M*	110.....	5327.24	3048.70	19.15	0.391	1	*E*
111.....	5327.27	3136.90	19.17	0.582	1	*C*	112.....	5324.19	3230.00	19.19	1.298	2	*EC*
113.....	5326.12	3428.50	19.19	1.264	3	*A*	114.....	5329.23	3447.00	19.21	0.583	1	*C*
115.....	5327.94	3559.20	19.21	...	0	*F*	116.....	5326.62	3432.50	19.24	0.584	1	*A*
117.....	5328.22	3721.70	19.26	...	0	*F*	118.....	5327.88	3429.80	19.27	...	0	*U*
119.....	5326.11	3347.50	19.27	...	0	*F*	120.....	5325.79	3125.60	19.27	...	0	*F*
121.....	5325.47	3535.00	19.28	0.948	1	*E*	122.....	5323.85	3413.40	19.30	0.570	2	*C*
123.....	5322.47	3116.80	19.30	1.440	4	*E*	124.....	5322.09	3037.40	19.30	...	0	*U*
125.....	5323.10	3253.10	19.31	1.009	4	*E*	126.....	5324.27	3017.20	19.31	1.301	5	*E*

TABLE 3—*Continued*

ID (D0K)	R.A.[a] (−0[h])	Decl. (−12°)	*K* (mag)	*z*	QC	SC	ID (D0K)	R.A.[a] (−0[h])	Decl. (−12°)	*K* (mag)	*z*	QC	SC
127.....	5323.24	3350.60	19.33	0.556	1	*B*	128.....	5322.88	3551.10	19.34	1.307	3	*A*
129.....	5329.21	3537.40	19.35	...	0	*U*	130.....	5320.96	3318.20	19.35	...	0	*F*
131.....	5323.83	3312.00	19.36	0.580	2	*C*	132.....	5323.76	3215.40	19.36	0.391	1	*E*
133.....	5323.64	3234.80	19.38	0.582	1	*C*	134.....	5321.16	3120.10	19.39	0.000	1	*M*
135.....	5324.48	3224.70	19.40	1.223	3	*A*	136.....	5324.83	3430.40	19.40	...	0	*F*
137.....	5323.66	3335.90	19.42	0.872	1	*EC*	138.....	5322.55	3502.00	19.43	0.428	1	*C*
139.....	5327.35	3245.10	19.43	0.573	3	*A*	140.....	5328.40	3647.70	19.44	0.772	1	*C*
141.....	5321.35	3124.30	19.45	...	0	*F*	142.....	5322.40	3627.80	19.46	0.761	1	*A*
143.....	5321.47	3319.80	19.47	0.750	3	*A*	144.....	5323.55	3430.00	19.51	0.370	1	*E*
145.....	5321.31	3158.60	19.51	0.581	1	*C*	146.....	5329.14	3551.90	19.51	...	0	*F*
147.....	5326.38	3116.20	19.52	0.415	1	*C*	148.....	5328.79	3508.10	19.52	...	0	*U*
149.....	5323.18	3711.10	19.53	0.269	1	*EB*	150.....	5321.73	3724.30	19.53	0.862	3	*C*
151.....	5322.98	3141.10	19.53	0.492	2	*C*	152.....	5328.83	3103.40	19.55	1.075	9	*A*
153.....	5326.38	3412.10	19.61	0.495	1	*C*	154.....	5329.14	3542.20	19.62	...	0	*U*
155.....	5321.35	3730.20	19.63	...	0	*F*	156.....	5324.38	3241.30	19.63	...	0	*F*
157.....	5323.71	3609.30	19.63	0.535	1	*C*	158.....	5328.04	3140.90	19.65	1.306	1	*E*
159.....	5321.43	3256.00	19.66	0.394	1	*E*	160.....	5327.69	3607.30	19.68	0.000	1	*M*
161.....	5324.43	3626.70	19.70	0.432	1	*C*	162.....	5322.76	3644.80	19.71	0.643	1	*C*
163.....	5324.72	3356.00	19.72	0.580	3	*A*	164.....	5328.66	3139.30	19.72	0.587	2	*C*
165.....	5328.48	3056.80	19.73	0.581	8	*A*	166.....	5326.60	3547.70	19.74	0.611	1	*EC*
167.....	5329.19	3351.70	19.74	0.442	1	*C*	168.....	5321.60	3204.00	19.74	...	0	*U*
169.....	5325.51	3530.70	19.76	...	0	*F*	170.....	5322.02	3547.60	19.76	0.533	1	*E*
171.....	5326.33	3020.90	19.77	0.345	1	*E*	172.....	5322.74	3209.00	19.77	0.974	9	*A*
173.....	5321.11	3243.50	19.81	...	0	*U*	174.....	5325.24	3640.70	19.83	0.968	5	*E*
175.....	5325.66	3434.70	19.84	0.939	4	*E*	176.....	5324.05	3536.10	19.85	...	0	*F*
177.....	5325.52	3559.00	19.86	...	0	*U*	178.....	5326.15	3359.60	19.88	0.745	3	*A*
179.....	5328.56	3618.20	19.89	0.763	2	*C*	180.....	5322.23	3650.60	19.90	...	0	*F*
181.....	5324.83	3254.70	19.91	1.040	9	*A*	182.....	5323.55	3357.60	19.92	1.137	3	*A*
183.....	5323.03	3437.60	19.92	0.922	1	*E*	184.....	5322.63	3509.80	19.92	0.622	1	*C*
185.....	5327.51	3611.40	19.92	0.975	1	*E*	186.....	5321.63	3020.50	19.95	...	0	*U*
187.....	5324.24	3630.60	19.96	0.344	1	*C*	188.....	5324.47	3617.90	19.98	1.218	2	*A*
189.....	5321.69	3303.70	19.98	0.490	4	*A*	450.....	5329.09	3030.30	18.12	0.000	1	*M*
956.....	5325.20	3615.60	19.48	0.000	1	*M*	494.....	5326.02	3534.90	18.91	...	0	*F*
504.....	5322.56	3252.30	19.06	...	0	*F*	506.....	5322.88	3546.60	19.07	...	0	*U*
507.....	5324.73	3408.00	19.12	1.002	4	*E*							
Supplemental Objects													
451.....	5322.12	3354.90	20.65	0.430	8	*A*	951.....	5329.56	3644.50	−20.00	0.440	1	*C*
953.....	5330.64	3632.40	−20.00	0.280	1	*E*	958.....	5327.06	3546.90	20.02	0.442	1	*C*
961.....	5318.41	3516.40	−20.00	0.000	1	*S*	968.....	5324.21	3325.70	20.58	0.000	1	*S*
971.....	5331.26	3212.00	−20.00	0.352	1	*E*	973.....	5330.40	3041.00	−20.00	0.340	1	*E*
980.....	5326.00	3157.01	20.20	0.437	1	*E*	982.....	5329.11	3020.81	20.45	1.420	9	*A*
983.....	5325.62	3504.53	−20.00	0.460	8	*A*	984.....	5321.50	3123.00	20.60	1.119	1	*E*
985.....	5321.16	3004.50	−20.00	0.773	4	*E*							

NOTE.—QC is the quality code described in § 3.3. SC is the spectral classification described in § 4.

[a] ID, right ascension, declination, and *R* magnitude from Pahre et al. 1998.

objects in the sample were used. There are four or more spectra for three of these galaxies.

4. GALAXY SPECTROSCOPIC CLASSIFICATIONS

A simple spectral classification was used (Table 2). "*E*" (emission) denotes a galaxy in which the emission lines dominate the spectrum, while the few extreme starburst galaxies that could be identified are denoted by "*B*." In the subsequent discussion, these two classes are usually referred to collectively as "*E*" (emission) galaxies. "*A*" (absorption) denotes an object where no emission lines are detected, while "*C*" (composite) is an intermediate case where both emission and absorption (usually 3727 and H + K) are seen. When both 3727 and 5007 Å emission lines are present, the object is denoted "*E*," or, if the absorption spectrum is also visible, "*EC*." The three AGNs are designated "*Q*." In addition, stars are classified according to the presence or absence of TiO bands (and/or CaH bands, for M subdwarfs) as "*M*" or "*S*" and, although there are no examples in the present sample, as "*W*" for white dwarfs.

The assignment of a spectral class to a galaxy will depend on its redshift and on the wavelength range covered by the observations. For example, a galaxy at low redshift with strong emission at 3727 and 5007 Å will be classified as "*E*," but the same object if seen at $z \sim 1.3$ when the 2800 Å region is observed in the optical will show no apparent emission features and will be listed as "*A*." This is particularly true for objects where the spectral coverage of the data did not extend to $\lambda > 7500$ Å. We emphasize that for $z < 0.9$, an "*A*" galaxy is an object that has a spectrum similar to that of local elliptical galaxies. But at higher redshift, only the strongest emission lines can be detected through the thicket

TABLE 4

DISTRIBUTION OF SAMPLE AMONG GALAXY SPECTRAL TYPES AND QUALITY CLASSES

Spectral Class	Number of Objects	Quality Class	Number of Objects
M	19	1	117[a]
S	5	2	14
Q	3	3	17
B	3	4	5
E	30	5	2
C	50	6	3
A	53	7	0
F	21	8	2
U	11	9	3
		0	32

[a] Includes 24 Galactic stars.

of night sky lines, and a much more diverse group of galaxies will be classified as "*A*" based on the presence of absorption lines in the 2500 Å region.

Figure 2 gives illustrative examples of the five spectral classes used for extragalactic objects. The spectrum of the second brightest AGN and the second brightest starburst galaxy are shown, while for the other three spectral classes, the spectrum of the fifth brightest galaxy (at *R*) assigned to that class is shown. The observed *R* magnitudes and *z* are indicated for each object. For the AGN and the spectral class "*C*" galaxy, the residuals from sky subtraction around the very strong night sky line at 5577 Å were removed by interpolation. The "*C*" galaxy shown has a rather weak 3727 Å emission line compared to most of the objects in this galaxy spectral class, but the distinction between "*C*" and "*A*" spectral classes is still clear from the relative strengths of absorption of H and K of Ca II, the Balmer lines, and the molecular bands of CH and CN in this spectral region. The spectrum of a somewhat more typical higher *z* "*C*" galaxy is also shown for comparison.

As will be discussed in Cohen et al. (1998), there are many galaxies in this field with $z \approx 0.58$. At this redshift, the

TABLE 5

MEDIAN REDSHIFT WITH MAGNITUDE

	R		*K*	
MAGNITUDE BIN	*N*	⟨*z*⟩	*N*	⟨*z*⟩
15.5–16.0	0		1	0.43
16.0–16.5	0		2	0.44
16.5–17.0	0		6	0.43
17.0–17.5	0		9	0.58
17.5–18.0	0		18	0.58
18.0–18.5	0		17	0.58
18.5–19.0	1	0.68	23	0.58
19.0–19.5	2	0.17	30	0.61
19.5–20.0	1	0.31	33	0.58
20.0–20.5	7	0.43		
20.5–21.0	4	0.43		
21.0–21.5	23	0.44		
21.5–22.0	23	0.58		
22.0–22.5	21	0.58		
22.5–23.0	28	0.64		
23.0–23.5	20	0.86		
23.5–24.0	5	0.76		
24.0–24.5	4	0.75		

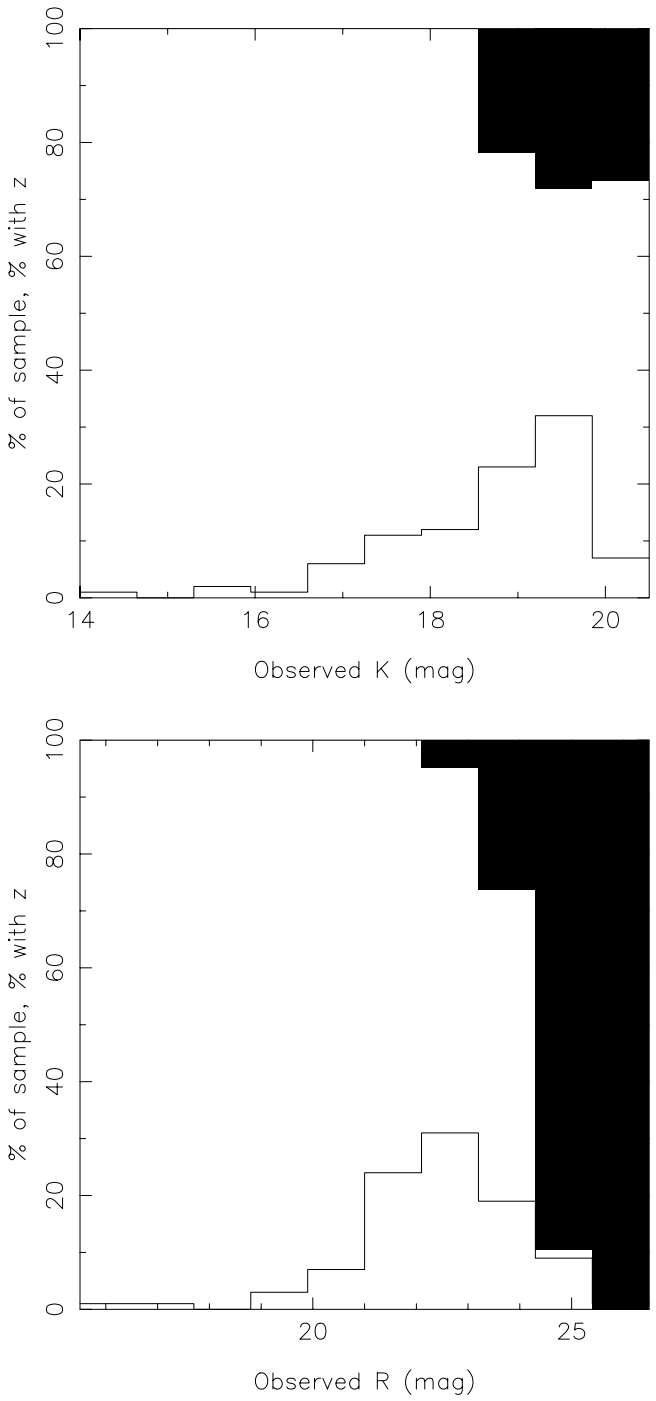

FIG. 3.—Histogram of the sample and the completeness of the redshifts are shown for the main sample. The filled area denotes the objects without redshifts. (*a*) *K* filter; (*b*) *R* filter.

3727 Å emission line of [O II], a key spectral type diagnostic, is observed at 5889 Å, where it overlaps the strong NaD doublet in emission from the night sky. Unless the emission from such a galaxy at 3727 Å [O II] is very strong, it may be lost in the uncertainty of subtracting away the much stronger night sky line. Thus, for this redshift only, the distinction between "*A*" and "*C*" spectral types has been made on the basis of the presence of the 3880 Å CN band and the G band of CH at 4300 Å. We assign such a galaxy a spectral class of "*A*" if those molecular bands are strong, while objects that show 4101 Å Hδ absorption in their spectra are

assigned the spectral class "$\mathscr{C}$." A check of 19 objects originally classified as "$\mathscr{A}$" in this redshift regime revealed three that had to be reclassified from "$\mathscr{A}$" to "$\mathscr{C}$" on this basis as well as three others too faint to determine which classification is most appropriate without the guidance of 3727 Å emission, which were left as "$\mathscr{A}$."

For the brighter part of this sample with high-precision spectra, considerably finer distinction among galaxy spectral classes is possible. A detailed discussion of the spectral features in the brighter galaxies of this sample is deferred to a future paper (Cohen et al. 1999).

5. REDSHIFTS FOR OBJECTS IN THE SAMPLE

Table 3 lists the object numbers, positions on the sky, measured K magnitudes (from Pahre et al. 1998), redshifts, spectral types, and quality classes for 195 objects in the main sample, followed by the 13 additional objects that constitute the total sample. Table 4 gives the distribution of objects in the main sample over the spectral and redshift quality classes.

Within the main sample, 84% of the objects have measured redshifts. The completeness is shown as a function of observed R and of observed K magnitude in Figure 3. As expected and supported by Figure 3, it is the R magnitude that primarily determines whether or not a redshift can be measured, rather than the K magnitude. The median R magnitude of the objects never observed is 24.6 mag, while the median R magnitude of the 21 objects that were observed, but for which no redshift was determined, is 24.3 mag. This latter group cannot contain any strong emission line objects with $z < 1.1$ otherwise their spectra would have already yielded redshifts.

All of the objects with redshifts in the main sample have R, I, and K magnitudes from the data of Pahre et al. (1998), but several are too faint to be detected in the available U, B, or V images.

The median redshift of the extragalactic objects in the main sample with measured z is 0.58. Even if it is assumed that all of the objects without redshifts are galaxies with $z > 1$, then the median redshift can only increase to $z_{\rm med} = 0.65$. Table 5 presents the median redshift for the extragalactic objects in the main sample in half-magnitude bins. The objects without redshifts have been ignored.

6. SUMMARY

This paper provides a description of the techniques for analyzing and characterizing the spectra obtained by the Caltech Faint Galaxy Redshift Survey. We have given here the basic observational results of our spectroscopic investigation of a complete sample of objects with $K_s < 20$ mag in a $2' \times 7\farcm3$ field at J005325+1234. Redshifts were successfully obtained for 163 of the 195 objects in the sample using the LRIS at the Keck Observatory. An analysis of these data, combined with the six-color photometric data of Pahre et al. (1998), for the extragalactic objects in this field will be given in Cohen et al. (1998).

The entire Keck/LRIS user community owes a huge debt to Jerry Nelson, Gerry Smith, Bev Oke, and many other people who have worked to make the Keck Telescope and LRIS a reality. We are grateful to the W. M. Keck Foundation, and particularly its late president, Howard Keck, for the vision to fund the construction of the W. M. Keck Observatory. J. G. C. is grateful for partial support from STScI/NASA grant AR-06337.12-94A. K. R. was supported in part by a Summer Undergraduate Research Fellowship at Caltech. R. D. B. acknowledges support under NSF grant AST95-29170. D. W. H. and M. A. P. were supported in part by Hubble Fellowship grants HF-01093.01-97A and HF-01099.01-97A from STScI (which is operated by AURA under NASA contract NAS5-26555).

REFERENCES

Bruzual, G., & Charlot, S. 1993, ApJ, 405, 538
Cohen, J. G., et al. 1999, in preparation
Cohen, J. G., Blandford, R., Hogg, D. W., Pahre, M. A., & Shopbell, P. L. 1998, ApJ, in press
Colless, M., & Boyle, B. 1998, Highlights Astron., 11, in press (astro-ph/9710268)
Cowie, L. L., Hu, E. M., & Songaila, A. 1995, Nature, 377, 603
Cowie, L. L., Songaila, A., Hu, E. M., & Cohen, J. G. 1996, AJ, 112, 839
Dey, A., Spinrad, H., Stern, D., Graham, J. R., & Chaffee, F. H. 1998, ApJ, 498, L93
Ellis, R. S. 1997, ARA&A, 35, 389
Ellis, R. S., Colless, M., Broadhurst, T., Heyl, J., & Glazebrook, K. 1996, MNRAS, 280, 235
Fanelli, M. N., O'Connell, R. W., Burstein, D., & Wu, C. C. 1992, ApJS, 82, 197
Francis, P. J., Hewett, P. C., Foltz, C. B., Chaffee, F. H., Weymann, R. J., & Morris, S. L. 1991, ApJ, 373, 465
Geller, M. J., et al. 1997, AJ, 114, 2205
Glazebrook, K., Offer, A. R., & Deeley, K. 1998, ApJ, 492, 98
Griffiths, R. E., et al. 1994, ApJ, 435, L19
Gunn, J. E., & Knapp, G. R. 1993, in ASP Conf. Ser. 43, Sky Surveys: Protostars to Protogalaxies, ed B. T. Soifer (San Francisco: ASP), 267
Huchra, J. P., Davis, M., Latham, D., & Tonry, J. 1983, ApJS, 52, 39
Kurtz, M. J., & Mink, D. J. 1998, PASP, 110, 934
Koo, D. C. 1998, in Redshift Surveys of the 21st Century, ed. A. Fairall (Kluwer: Dordrecht), in press
Koo, D. C., & Kron, R. G. 1992, ARA&A, 30, 613
Lilly, S. J., Hammer, F., LeFèvre, O., & Crampton, D. 1995a, ApJ, 455, 75
Lilly, S. J., LeFèvre, O., Crampton, D., Hammer, F., & Tresse, L. 1995b, ApJ, 455, 50
Madau, P., Pozzetti, L., & Dickinson, M. 1998, ApJ, 498, 106
Oke, J. B. 1990, AJ, 99, 1621
Oke, J. B., et al. 1995, PASP, 107, 307
Pahre, M. A., et al. 1998, ApJS, submitted
Shectman, S. A., Landy, S. D., Oemler, A., Jr., Tucker, D. L., Lin, H. A., Kirshner, R. P., & Schechter, P. L. 1996, ApJ, 470, 172
Shortridge, K. 1988, The Figaro Manual, Version 2.4 (Pasadena: Caltech)
Skrutskie, M., et al. 1999, in preparation
Steidel, C. C., Giavalisco, M., Pettini, M., Dickinson, M., & Adelberger, K. L. 1996, ApJ, 462, L17
Vettolani, G., et al. 1997, A&A, 325, 954
Wainscoat, R. J., & Cowie, L. L. 1992, AJ, 103, 332